

# The hydrometallurgical processing of a low-grade manganese ore from the Northern Cape, South Africa

L. Mukumbi<sup>1</sup>, C. Saguru<sup>1</sup>, and C.J. N. Dempers<sup>2</sup>

<sup>1</sup>CM Solutions, South Africa

<sup>2</sup>PRODEO Consulting, South Africa

Preliminary test work was conducted for the development of a hydrometallurgical process flowsheet to recover manganese from a low-grade manganese oxide ore. The flowsheet under investigation consists of milling, reductive acid leaching, removal of impurities by precipitation, and crude manganese precipitation. The impure manganese precipitate is then re-dissolved, prior to further solution purification and recovery of manganese by crystallisation as high purity manganese sulphate monohydrate. The test work included mineralogical analyses and chemical characterisation of two samples that were obtained from the Kitso Mine in the Northern Cape, South Africa. Leaching, removal of impurities by precipitation and crude manganese carbonate precipitation were also investigated. The results of the test work indicated the viability of applying a hydrometallurgical processing flowsheet on a low-grade manganese ore. A set of optimal processing parameters were then established and are discussed, together with the implications of the current test work results on the design of a manganese refinery.

## INTRODUCTION

South African deposits account for approximately 40% of the known global manganese (Mn) reserves (Mineral Commodity Summaries, 2021). The Northern Cape province hosts the majority of these deposits, in an area known as the Kalahari basin. The mineralogy of these deposits shows considerable mineral species intergrowth, as well as Mn displacement of other elements. (Kleyenstuber, 1984). This is likely caused by the hydrothermal nature of the deposits, and presents challenges with both upfront preconcentration steps, as well as the hydrometallurgical processing methods to achieve a high purity Mn product.

Mn demand in the green energy industries has been steadily increasing. The battery storage market is one such use case where demand for Mn is expected to increase, driven by growth in the electric vehicle (EV) market. Mn is used as a substitute for cobalt (Co) to reduce cathode manufacturing costs (Yi *et al.*, 2023). The precursors are usually high purity manganese sulphate monohydrate (HPMSM) or electrolytic manganese dioxide which are obtained through a series of hydrometallurgical purification steps.

## OVERVIEW OF THE HYDROMETALLURGICAL RECOVERY OF MANGANESE

The hydrometallurgical processing of Mn has traditionally been conducted by initially roasting the Mn ore in the presence of a suitable reducing agent. Coal (Harris *et al.*, 1977), graphite, carbon monoxide, pyrite, elemental sulphur (Zhang *et al.*, 2013) or biomass (Cheng *et al.*, 2009) have been investigated in prior works, to convert the oxidised Mn mineral (usually in the +4 oxidation state) to acid soluble Mn(II) oxide, prior to acid leaching. Mn ores typically have extremely complex mineralogy due to Mn stability in various oxidation states, resulting in substantive substitution of Mn with metals like Al, and Fe. Mn leaching has therefore been traditionally conducted after reductive roasting, to ensure that all the Mn which was present in the insoluble +4 oxidation state was reduced to the more soluble +2 oxidation state.

Recent approaches have focused on purely hydrometallurgical flowsheets, by-passing the reductive roasting step. Mn direct leaching has been investigated; employing reducing, acidic conditions that provide the necessary thermodynamic conditions for soluble  $\text{Mn}^{2+}$  stability, as predicted by the Pourbaix diagram (Toro *et al.*, 2021) in Figure 1.

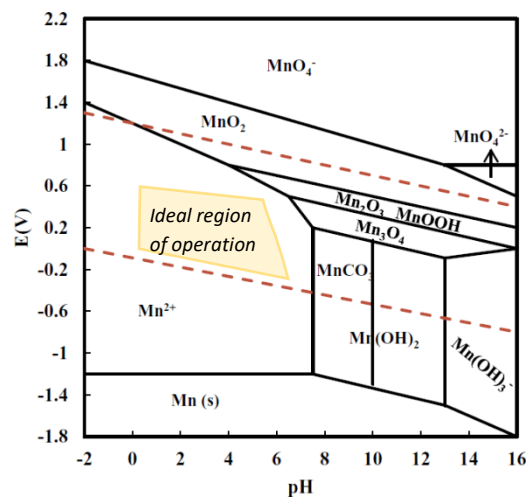


Figure 1. Pourbaix diagram for manganese (Toro *et al.*, 2021).

Mn is then recovered from solution either as a salt or metal by using various processes such as evaporative crystallisation, precipitation, and electrowinning. Battery grade Mn sulphate has extremely low tolerances for various base metal impurities, especially Fe, Ca, Cu, Cr, Mg, Na, Pb and Zn. The level of metal impurities reporting to the final Mn product depends on the recovery route that is eventually chosen.

In this work, Mn was recovered by employing a flowsheet that consisted of reductive acid leaching with  $\text{SO}_2$  gas as a reducing agent, followed by Fe removal using limestone. Mn precipitation using  $\text{NH}_4\text{HCO}_3$  was then carried out on the solution from Fe precipitation to produce a crude Mn carbonate product.

The precipitated Mn carbonate product is then redissolved, and the resulting solution purified by ion exchange and/or precipitation, prior to crystallisation to obtain final HPMSM salt. A block diagram of the flowsheet is presented in Figure 2.

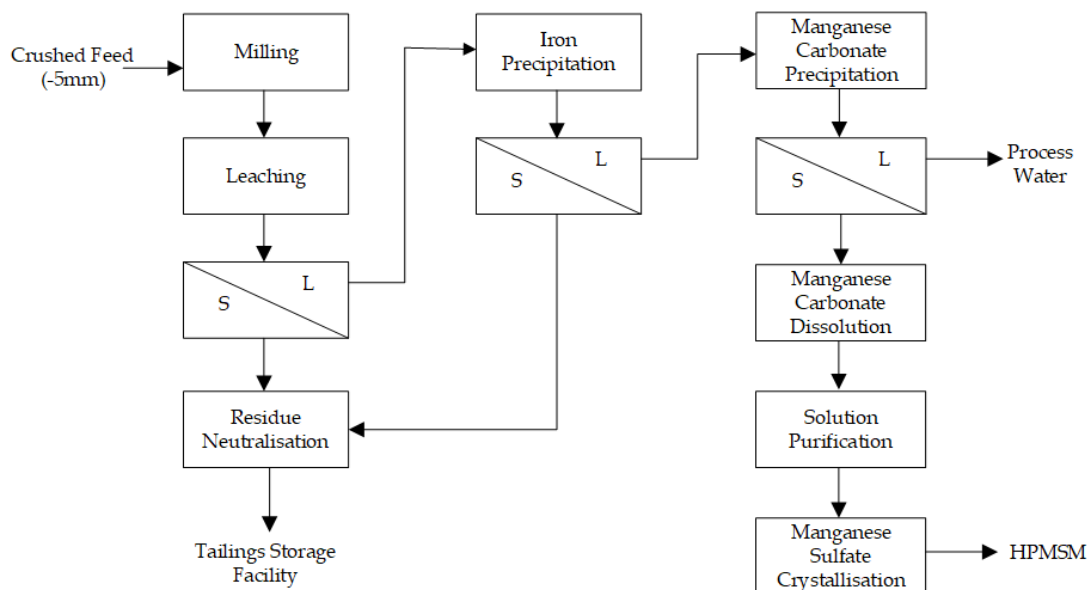


Figure 2. Mn process block flow diagram.

## DESCRIPTION OF TEST WORK METHODOLOGIES

### Sample Characterisation

Samples for the test work were received from Kitso mine in the Northern Cape, with a particle size distribution of approximately 100% <math>-100\text{ mm}</math>. The as received sample was crushed to 100% passing 3.35 mm and 100% passing 1.18 mm using a jaw crusher to obtain samples for bond ball mill index tests, milling curve and for the mineralogical characterisation test work, which was conducted at SJT MetMin Laboratories.

A sub sample was also pulverised and sent for head grade analysis, by peroxide fusion and base metal analysis using inductively coupled plasma optical emission spectroscopy (ICP-OES).

### Leaching test work methodology

Based on preliminary financial evaluations it was established that the parameters most affecting the project economics are leach efficiency and acid consumption. The main variables that can be manipulated to optimise these factors in the leach are pH, grind size and temperature. To this end, a series of tests were conducted, to establish the effect of pH, temperature and grind size. A further optimising test was then conducted at higher pulp density, in order to increase Mn concentration in the pregnant leach solution (PLS). Table 1 presents a summary of the test work conditions that were investigated for leaching the Mn ore sample.

In order to conduct the actual leach tests, the leach vessel was charged with the feed solution, agitated and temperature increased until reaching the target temperature. The feed solids required were weighed and pulped into the feed solution. The pH of the solution was adjusted and controlled at the targeted pH within the first half hour of the reaction, by the addition of  $\text{H}_2\text{SO}_4$  using a peristaltic pump.

At target pH, sulphurous acid was then added as a reductant at a constant flowrate, using a peristaltic pump. The target was always to achieve a final redox potential of below 350 mV vs. Ag/AgCl electrode. All redox potentials reported in this work were at test temperature and measured relative to the saturated Ag/AgCl electrode. Parameters such as pH and redox potential were recorded on a half hourly basis for the first two hours and hourly thereafter for a total of six hours. The volume of acid and reductant added were also monitored. Kinetics samples were taken during the tests, centrifuged and sent for analysis.

Table 1. Summary of leaching conditions

Description	Units	Value
pH	-	1.5, 1.8, 2
Temperature	°C	50, 70 & 90
Size fraction	$\mu\text{m}$	P <sub>75</sub> ~75, 150, 250
Leach pulp density	% m/m	20 & 40
Redox potential (vs. Ag/AgCl)	mV	Below 350 mV
Residence time	h	6
Reductant	-	Sulphurous acid
Sulphuric acid concentration for pH control	g/L	300

On completion of the test, the slurry was filtered, the filtrate volume noted, and the resultant cake dried. All solution samples collected were then analysed by ICP-OES. Solid samples were initially pulverised before undergoing peroxide fusion and base metal analysis by ICP-OES.

### Iron and Manganese precipitation test work methodology

The main objective of these tests was to selectively precipitate Fe from the Mn rich solution by using oxidative Fe precipitation, followed by precipitating Mn as a crude carbonate from the Fe free barren.

A pH S-Curve was initially conducted to determine a suitable precipitation pH for Fe without significant losses of the Mn from the PLS obtained during leaching. The precipitation tests were done at a temperature of 70°C, using 10% limestone for Fe precipitation. Once the target pH was attained, the reaction was allowed to proceed, typically for about 15 minutes, to allow time for the pH to stabilise, after which a sample was taken for analysis. Process parameters such as pH, ORP, and temperature were periodically recorded. The results from the S-Curve tests were used to select a terminal pH for a confirmatory Fe precipitation test, to generate Fe barren solution for further Mn precipitation tests.

A similar approach, of conducting an S-Curve test first, followed by bulk Mn precipitation, was adopted to determine Mn precipitation conditions. The pH controlling reagent for the Mn precipitation, however, was 20% m/m ammonium bicarbonate (NH<sub>4</sub>HCO<sub>3</sub>) solution. This reagent was selected to avoid introducing contaminant ions, e.g. Na, Ca, Mg.

Upon completion of the tests (i.e., S-Curve tests and confirmatory precipitation tests), the slurry was filtered, and the filtrate volume recorded, and samples sent for base metal analysis by ICP-OES.

## EXPERIMENTAL RESULTS AND DISCUSSION

### SAMPLE CHARACTERISATION

#### Chemical and Mineralogical analysis

Table 2. Average head assay composition for the Mn-ore sample

Element	Al	Ca	Co	Cr	Cu	Fe	Mg	Mn	Si	Zn
Head assay	4.92%	0.67%	0.01%	0.11%	0.02%	20.64%	0.26%	22.56%	3.29%	0.01%

Chemical analysis indicated that the sample has a Mn grade of approximately 23% as presented in Table 2. Mineralogical analysis of the Kitso sample indicated that the Mn containing phases are cryptomelane, (K(Mn<sup>4+</sup>,Mn<sup>2+</sup>)<sub>8</sub>O<sub>16</sub>) and Bixbyite ((Mn,Fe)<sub>2</sub>O<sub>3</sub>), which together account for approximately 47% by mass of the ore as illustrated in Table 3.

The sample also assayed 21% Fe, which was primarily hosted in hematite. Hematite accounts for approximately 41% of the ore. Table 3 summarises the approximate compositions of the constituent phases in the Mn ore sample, as obtained from XRD characterisation.

Table 3. Semi-quantitative composition for the Mn-ore sample

Mineral Phases	Units	Mn-Ore
Hematite ( $\text{Fe}_2\text{O}_3$ )	%	40.9
Cryptomelane ( $\text{K}(\text{Mn}^{4+}, \text{Mn}^{2+})_8\text{O}_{16}$ )	%	32.7
Bixbyite ( $(\text{Mn}, \text{Fe})_2\text{O}_3$ )	%	15.7
Todorokite ( $(\text{Na}, \text{Ca}, \text{K})_2(\text{Mn}, \text{Mn})_6\text{O}_{12.3-5.5}(\text{H}_2\text{O})$ )	%	5.8
Diaspore ( $\text{AlO}(\text{OH})$ )	%	2.5
Quartz ( $\text{SiO}_2$ )	%	2.4
<b>Total</b>	%	<b>100.0</b>

AutoSEM imaging analysis was also conducted on the sample. Imaging analysis and elemental mapping indicated that the Mn-phases and the gangue phases are intensely intergrown with one another as shown in Figure 3.

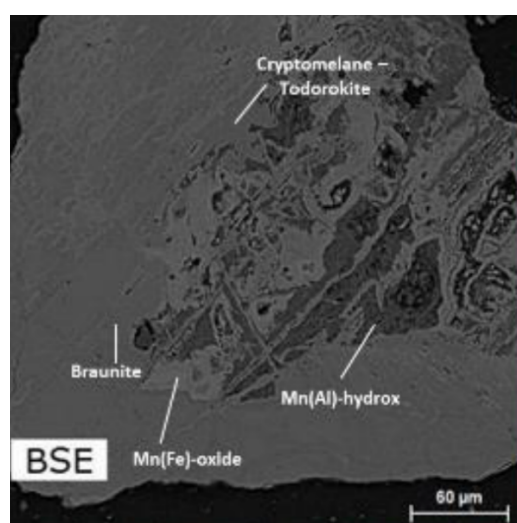


Figure 3. BSE image overview indicating the complicated intergrowth between the main Mn phases and the gangue phases present.

#### Milling curve (Grind calibration) and bond work index tests

Grind calibration (milling curve) tests were conducted to determine the required times to mill in the laboratory rod mill, in order to obtain targeted P80 passing sizes for the grind size selection leaching tests. Bond work index tests were also conducted to obtain the sample's ball mill work index, which provides an indication of energy consumption for milling. The results of these tests are presented in Table 4, indicating that the sample has a 'very high' hardness with a work index of 21.5 kWh/t.

Table 4. Bond work index tests results

	G (g/rev)	Wi (kWh/t)	P (d80 prod)	F (d80 feed)	Energy (kWh/t)
<b>Bond work test</b>	0.9	21.5	89.6	2204.7	18.2

Where: G (g/rev)= average grams of undersize material produced per revolution for the last three cycles,  $W_i$  (kWh/t)= Bond Work Index (kWh/t), P (d80 product)= 80% passing size of the final undersize ( $\mu\text{m}$ ), F (d80 feed) = 80% passing size of the new feed, Energy (kWh/t) - Energy required to mill 1 ton.

## LEACHING TESTS RESULTS

The effects of grind size, solids content, temperature and slurry pH on the leaching of Mn were investigated using the one-factor-a-time methodology.

### Effect of pH

The effect of pH was investigated over three different target pH values of 1.5, 1.8 and 2.0. The temperature was fixed at 90°C, utilising ore milled to a P80 -75 µm at an initial pulp density of 20% (m/m). The results for these tests are shown in Table 5 and Figure 4. Increasing the pH from pH 1.5 to pH 2.0 resulted in a decrease in the Mn leach efficiency from 93% to 88%, with an associated decreasing acid consumption from 336 kg/ton to 156 kg/ton. Leaching of Mn is favoured by acidic conditions and the availability of more acid (at lower pH) was expected to favour leaching kinetics and leaching extent.

Table 5. Effect pH -leach tests work results

	Units	Test 1	Test 2	Test 3
pH value		1.5	1.8	2.0
Leach efficiency	%	93	84	88
Acid consumption	kg/ton	336	252	156
Final Eh	mV	351.6	254.9	178.6
Mn concentration in filtrate	mg/L	23615	26879	20824

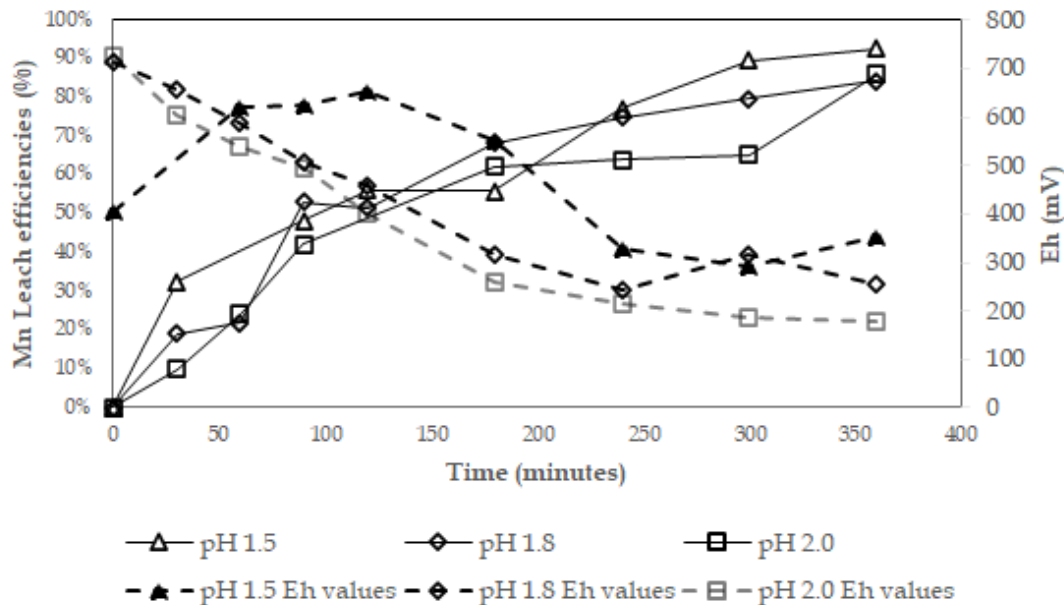


Figure 4. Manganese kinetic leach efficiency curves at pH of 1.5, 1.8 and 2.0.

### Effect of temperature

The effect of temperature on the leaching of Mn was also evaluated on material milled to a P80 - 75 µm, targeting a pH of 1.5 at an initial pulp density of 20% (m/m). A summary of the leaching test results is shown in Table 6 and in Figure 5. Decreasing the leaching temperature from 90°C to 50°C resulted in a decrease in the Mn leaching efficiency from 93% to 84%

Table 6. Effect of temperature – leach tests work results

	Units	Test 1	Test 2	Test 3
Temperature	°C	90	70	50
Leach efficiency	%	93	86	84
Acid consumption	kg/ton	336	270	276
Final Eh	mV	351	108	357
Mn concentration in filtrate	mg/L	23615	20162	16326

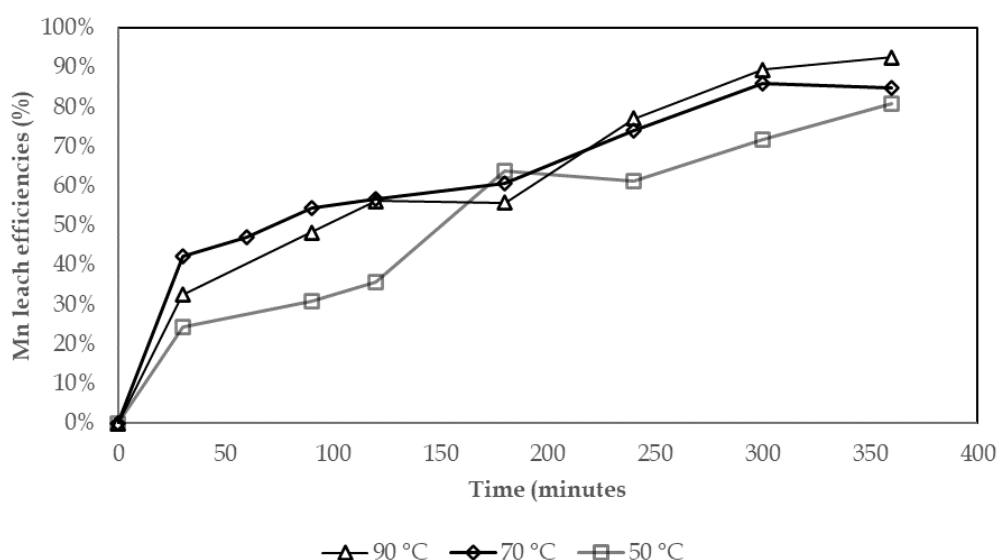


Figure 5. Effect of temperature – manganese kinetic leach at temperature of 50, 70 and 90°C.

#### Effect of grind size

The results from previous tests indicated that Mn leaching was favoured by lower pH values and higher temperature. Further leaching tests to investigate the effect of grind size were therefore conducted at a pH of 1.5 and a temperature of 90°C. The results from these tests are summarised in Table 7 and in Figure 6. Increasing the grind size from 150 µm to 250 µm decreased the recovery of Mn from 93% to 84% (m/m). This result could be attributed to the intense intergrowth of Mn phases in gangue minerals as illustrated earlier in Figure 3, resulting in physical locking of the Mn minerals at coarser grind sizes. Leaching at a P80 -75 µm and -150 µm attained a similar leaching efficiency (93%), indicating no further benefits accruing from grinding finer than 150 µm. In contrast, finer grinding did in fact result in a higher acid consumption of 336 kg/ton, compared to 228 kg/ton, likely due to higher liberation of gangue minerals at the lower grind size. Considering the costs of acid and energy required to mill more finely, the grind size with a P80 -150 µm is the more favourable particle size.

Table 7. Effect grind size-leach tests results

	Units	Test 1	Test 2	Test 3
Particle size (P80)	µm	75	150	250
Leach efficiency	%	93	93	84
Acid consumption	kg/ton	336	228	108
Final pH		1.35	1.45	1.50
Final Eh	mV	351	266	180
Mn concentration in filtrate	mg/L	23615	18803	18561

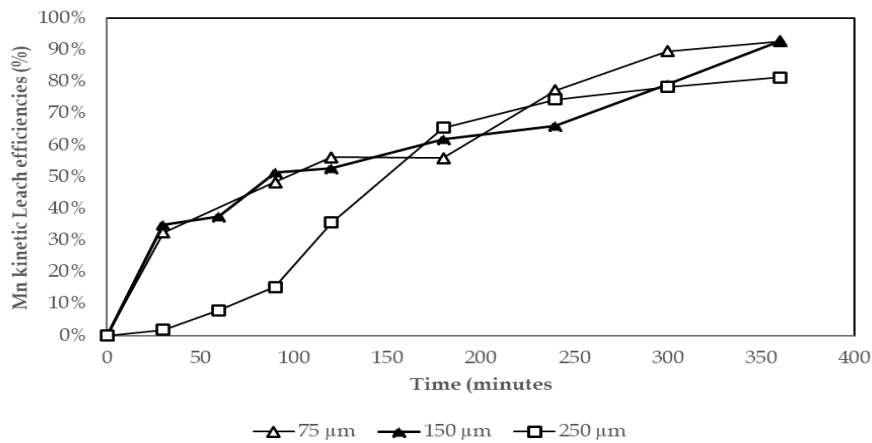


Figure 6. Effect of grind size - manganese kinetic leach at 75 µm, 150 µm and 250 µm.

### Effect of solids content

The results discussed above showed that the final Mn concentration in the leach liquor was consistently below 40 g/L. It was decided to increase the initial solids content from 20% (m/m) to 40% (m/m) in an attempt to increase the final Mn concentration in the leach liquor. The results from these tests are presented in Table 8 and in Figure Figure 7. The Mn concentration in the final filtrate was doubled to 46 g/L by increasing the initial pulp density from 20% to 40% (m/m). However this resulted in a decrease in Mn recovery from 93% to 81%. The poor leaching of Mn at 40% solids content could have been as a result of insufficient utilisation of reagents, as the redox potential on completion of the test was still above the value of 350 mV at test termination. More tests need to be done at longer residence times to determine the impact of residence time on leaching efficiency at higher % solids.

Table 8. Effect solids content – leach tests work results

	Units	Test 1	Test 2
Target initial % solids	% w/w	20	40
Leach efficiency	%	93	81
Acid consumption	kg/ton	336	210
Final pH		1.35	1.47
Final Eh	mV	351	386
Mn concentration in filtrate	mg/L	23615	46061

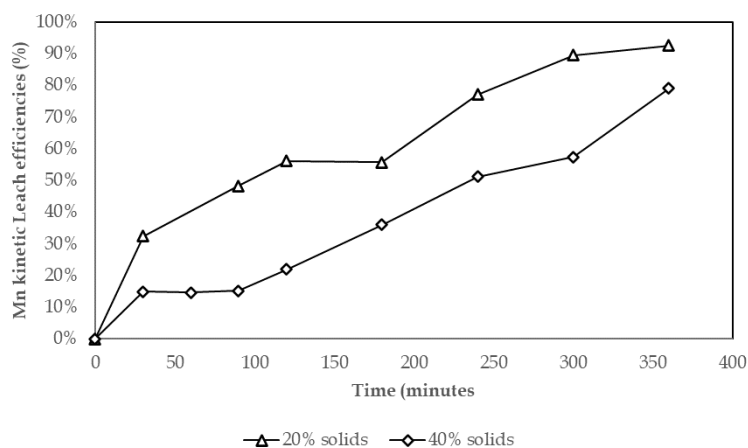


Figure 7. Effect of solids content – manganese kinetic leach at solids content of 20% and 40%.



## Fe PRECIPITATION RESULTS

The purpose of the Fe precipitation tests was to determine the optimum pH for removing the Fe, whilst minimising Mn losses. This was determined by means of a pH vs metal precipitation S-Curve, using 10% limestone as pH control reagent. A confirmatory precipitation test was then conducted, employing insights from the pH S-Curve test. This test also served to generate Fe free liquor for the Mn precipitation tests. Table 9 presents a summary of results from these two tests.

The Fe precipitation tests were done on leach liquor which had initial Mn and Fe concentrations of 25 g/L and 1.6 g/L respectively. The pH S-Curve, presented in Figure 8 indicated that quantitative removal of Fe could be attained at a terminal pH of 5.5, with just a 3% Mn loss. The confirmatory test was then conducted to a pH of 5.0, attaining 96% Fe precipitation, with Mn loss of 4%.

Table 9. Summarised Fe precipitation results

	<i>Units</i>	<i>Fe-PPT-1</i>	<i>Fe-PPT-2</i>
<b>Test description</b>		<b>Fe precipitation S-Curve</b>	<b>Confirmatory Fe precipitation</b>
Fe precipitation efficiency	%	100	96
Mn loss/precipitation	%	3	4
Final pH		5.5	5.0
Mn head assay	mg/L	25029	26251
Mn in final filtrate	mg/L	20910	21707
Fe head assay	mg/L	1586	1654
Fe in final filtrate	mg/L	0.14	70

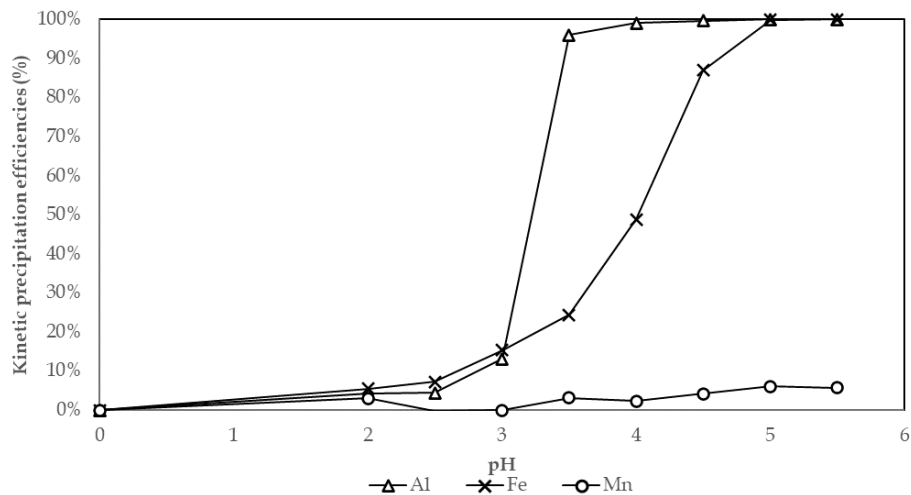


Figure 8. Fe precipitation efficiency S-curve.

## Mn PRECIPITATION RESULTS

The purpose of the Mn precipitation tests was to determine the optimum conditions for generating an impure Mn product for further purification test work. The Mn precipitation tests were carried out on solution after Fe precipitation. Table 10 presents a summary of the results, indicating that the solution that was used had Mn concentrations of 17 g/L and 22 g/L, while Fe assayed 56 and 52 mg/L. The Mn precipitation tests were conducted in a similar manner to the approach used for Fe precipitation, with

an S-Curve first, followed by a confirmatory test. The Mn precipitation was conducted using ammonium bicarbonate solution, from a solution with initial pH of 4.6.

The Mn precipitation S-Curve test indicated that a precipitation efficiency of >99% (m/m) was attained at terminal pH of 7.6. This was successfully replicated in a batch confirmatory test, wherein Mn precipitation was also quantitative, attaining a terminal Mn concentration less than 3 mg/L. Due to the high terminal pH values, residual Fe was also polished out and reported into the Mn crude product as indicated in Figure 8.

Table 10. Summarised Mn precipitation results

Test ID	Units	Mn-PPT-1	Mn-PPT-2
Test description		Mn precipitation S-Curve	Mn precipitation confirmatory test
Mn in the precipitate	%	45	45
Mn precipitation efficiency	%	100	100
Mn head assay	mg/L	22646	16901
Mn in final filtrate	mg/L	0.16	2.76
Final pH		7.6	7.6
Fe head assay	mg/L	56	52
Fe in final filtrate	mg/L	0.15	1.68
Fe in final precipitate	%	0.16	0.01

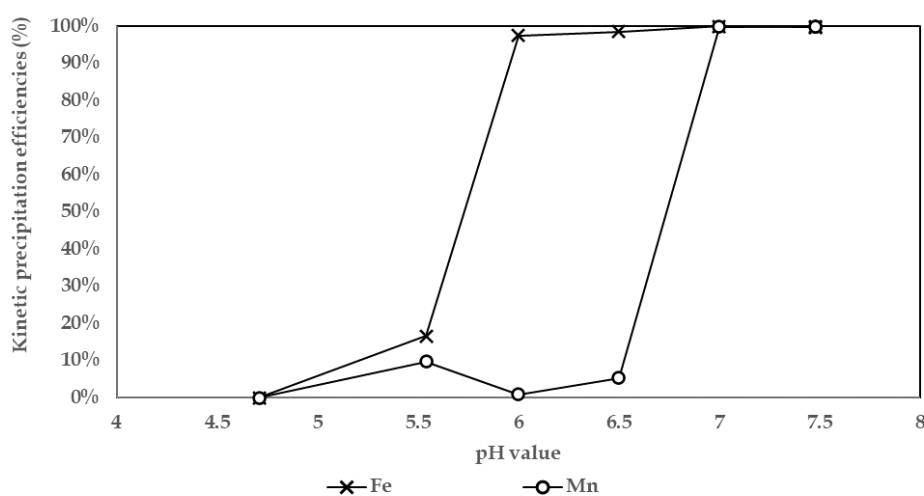


Figure 9. Mn precipitation efficiency S-curve.

### **Mn PRECIPITATION PRODUCT CHARACTERISATION**

The precipitates produced in Test 1 and Test 2 had Mn contents of 45.31% (m/m) and 44.86% (m/m) as shown in Table 11. Impurity elements are also reported in Table 11, indicating that precipitation alone was not adequate to generate a product of sufficient purity. It is therefore suggested that a redissolution step – followed by impurity removal using successive ion exchange and precipitation – is employed prior to Mn product recovery by crystallisation. This was however not tested in this current work.

Table 11. Final Mn precipitate chemical composition

Element	Al	Ca	Co	Fe	Mg	Mn	Ni
Unit	mg/kg	% m/m	mg/kg	mg/kg	mg/kg	% m/m	mg/kg
Composition	45.1	1.3	294.1	56.9	1114	45.1	148.6

## DESIGN CONSIDERATIONS

Based on the test work and literature review, it is evident that the flowsheet shown in Figure 1 is feasible for producing a crude Mn product from a processing perspective. Design criteria for the process plant were therefore developed as shown in Table 12.

The leach conditions were selected to optimise the Mn recovery and acid utilisation. The Fe precipitation criteria were selected to maximise Fe rejection and minimise Mn losses. The conditions for the Mn precipitation were selected to maximise the impurity rejection but optimise the Mn recovery.

Additional test work is required to determine:

- Optimise the leach solids composition (% solids) and residence time
- Residence time required for Fe precipitation
- Residence time required for Mn precipitation and
- Efficiency and kinetics for Mn carbonate re-dissolution.

Further test work to obtain a pure Mn solution, prior to crystallisation of HPMSM, is also essential. Purification can be conducted by using ion exchange and/or fluoride precipitation of PLS obtained from dissolution of the crude Mn carbonate. Calcining the crude Mn product, before reductive dissolution of the calcined product to produce a relatively pure PLS is another optional process route. These approaches should be compared in terms of anticipated project economics and technical feasibility.

Table 12. Process plant design criteria

Description	Units	Value
<b>Leaching</b>		
Leach feed solids composition	% (w/w)	20
Leach feed particle size distribution (P80)	$\mu\text{m}$	150
Residence time	<i>h</i>	6
pH		1.5
Lixiviant		98% H <sub>2</sub> SO <sub>4</sub>
Acid consumption	kg/t feed	270
Target ORP (vs. Ag/AgCl)	mV	350
Reducing Agent		SO <sub>2</sub> (g)
Operating temperature	°C	90
Leaching extent		
Mn	%	93
Fe	%	32
Mass loss in leaching	%	35
<b>Fe Precipitation</b>		
Final pH		5.5
Precipitation agent		20% limestone slurry
Precipitation extent		
Mn	%	3
Fe	%	99.9

Description	Units	Value
<b>Mn Precipitation</b>		
Final pH		7.5
Precipitation agent		NH <sub>4</sub> HCO <sub>3</sub>
Precipitation extent		
Mn	%	100
Fe	%	100

## CONCLUSIONS AND RECOMMENDATIONS

The test work showed that it is possible to leach ore from the Kitso mine with a reductive leach, followed by removal of the Fe using partial neutralisation with limestone before the precipitation of a relatively pure Mn carbonate product with ammonium bicarbonate. The Mn carbonate product requires further processing in order to produce HPMSM.

The Mn leaching test work established that pH, temperature, grind size and solids content had major impacts on the leaching of Mn. The Mn leach efficiency increased with a decrease in pH and an increase in temperature. Leaching was also improved by grinding more finely, but only up to a P80 -150 µm, as finer grinding to a P80 -75 µm did not translate into further improvements in leaching efficiency. Mn leaching was also negatively affected by increasing initial pulp density for leaching.

Overall, the results of the test work and the design criteria developed in this study can be used to establish the design parameters for an effective hydrometallurgical processing circuit to produce HPMSM. The design can be optimised further to ensure that the circuit operates at maximum efficiency with minimal environmental impact.

It is recommended that this process design is developed further, and additional test work is conducted. The MnCO<sub>3</sub> dissolution, solution purification and HPMSM crystallisation test work are critical to establishing a design for the process plant to produce HPMSM.

## REFERENCES

- Cheng, Z., Zhu, G., Zhao, Y., 2009. Study in reduction-roast leaching Mn from low-grade manganese dioxide ores using cornstalk as reductant. *Hydrometallurgy* 96, 175–179. <https://doi.org/10.1016/j.hydromet.2008.08.004>
- Harris, M., Meyer, D.M., Auerswald, K., 1977. The production of electrolytic manganese in South Africa. *J. South Afr. Inst. Min. Metall.* 77, 137–142.
- Kleyenstuber A.S.E., 1984. The mineralogy of the manganese bearing hotazel formation of the proterozoic transvaal sequence in Griqualand West South Africa
- Mineral Commodity Summaries, 2021
- Toro, N., Rodríguez, F., Rojas, A., Robles, P., Ghorbani, Y., 2021. Leaching manganese nodules with iron-reducing agents - A critical review. *Miner. Eng.* 163, 106748. <https://doi.org/10.1016/j.mineng.2020.106748>
- Yi, H., Liang, Y., Qian, Y., Feng, Y., Li, Z., Zhang, X., 2023. Low-Cost Mn-Based Cathode Materials for Lithium-Ion Batteries. *Batteries* 9, 246. <https://doi.org/10.3390/batteries9050246>
- Zhang, Y., You, Z., Li, G., Jiang, T., 2013. Manganese extraction by sulfur-based reduction roasting–acid leaching from low-grade manganese oxide ores. *Hydrometallurgy* 133, 125–132. <https://doi.org/10.1016/j.hydromet.2013.01.003>



## **Collins Tatenda Saguru**

Senior Projects Engineer  
CM Solutions Metlab

Collins possesses vast experience in process development of flowsheets for recovery of base and precious metals. He has also acquired exposure to optimising existing plant installations through analysis of plant data and overseeing test work to investigate flowsheet optimisation initiatives. Collins' unit process experiences are in comminution characterisation, flotation, leaching (heap and agitated), precipitation, solvent extraction and ion exchange, with some exposure to thickening and rheology investigations.

